

Overview of ELM control by low n magnetic perturbations on JET

Y. Liang¹, H. R. Koslowski¹, S. Jachmich², E. Nardon³, A. Alfier⁴, T. Eich⁵, C. Gimblett³, C. Giroud³, G. Maddison³, P. T. Lang⁵, M. P. Gryaznevich³, D Harting¹, S. Saarelma³, Y. Sun¹, R. Wenninger⁵, C. Wiegmann¹ and JET-EFDA contributors*

JET-EFDA, Culham Science Centre, OX14 3DB, Abingdon, UK

¹Association EURATOM-FZJ, Forschungszentrum Jülich GmbH, Institute of Energy Research IEF-4: Plasma Physics, Partner in the Trilateral Euregio Cluster, 52425 Jülich, Germany;

²Association EURATOM-Belgian State, Koninklijke Militaire School - Ecole Royale Militaire, B-1000 Brussels Belgium;

³EURATOM-UKAEA Fusion Association, Culham Science Centre, OX14 3DB, Abingdon, OXON, UK;

⁴Associazione EURATOM-ENEA sulla Fusione, Consorzio RFX Padova, Italy;

⁵Max-Planck-Institut für Plasmaphysik, EURATOM-Assoziation, D-85748 Garching, Germany;

Introduction Active control of edge localized modes (ELMs) by externally applied fields offers an attractive method for next-generation tokamaks, e.g. ITER. The previous experiments on JET and DIII-D have shown that type-I ELMs can be controlled by applying static external magnetic perturbation fields [1-3]. On JET, when a low n (1, 2) field with amplitude of a few Gauss at the plasma edge ($\sqrt{\psi_N} > 0.95$) is applied during the stationary phase of a type-I ELMy H-mode plasma, the ELM frequency rises by a factor of ~ 4 -5 and follows the applied perturbation field strength. This allows for ELM control in a wide range of plasma parameters. The frequency of the mitigated ELMs is proportional to the input heating power similarly to Type-I ELM, but the controlled ELMs have a higher frequency and are smaller in amplitude.

In this paper, an overview of the key physics issues related to ELM control with magnetic perturbation fields is given from the experimentalist's point of view including edge magnetic ergodisation, density pump-out effect, non-resonant magnetic plasma rotation braking and multi-resonance effect in ELM frequency.

Experimental results An overview on an ELM control pulse is shown in figure 1. The pulse had a toroidal magnetic field of $B_0 = 2.1$ T and a plasma current of $I_p = 1.8$ MA, corresponding to an edge safety factor of $q_{95} = 4.0$. In these experiments, the type-I ELMy H-mode plasma with a high triangularity shape was sustained by neutral beam injection (NBI) with an input power of 7.5 MW for ~ 10 s. The electron collisionality at the pedestal is ~ 0.2 . No additional gas fuelling was applied during the H-mode phase. The $n = 1$ perturbation field created by the EFCCs had a flat-top with $I_{\text{EFCC}} = 32$ kAt for 2 s, which is about 8 energy confinement times. The Chirikov parameter calculated using the experimental parameters and the vacuum approximation of the perturbation field is about 0.85 at $\sqrt{\psi_N} > 0.95$. It is larger than 1 near the separatrix, which indicates that the islands chains already overlap. During the EFCC phase the D_α signal measuring the ELMs showed a strong reduction in amplitude. The ELM frequency increased from ~ 30 Hz to ~ 120 Hz, while the periodic energy loss due to the ELM crashes normalized to the total stored energy, $\Delta W/W$, measured by a fast diamagnetic loop, indicates a strong reduction from $\sim 8\%$ to

* See the Appendix of F. Romanelli et al., Proceedings of the 22nd IAEA Fusion Energy Conference, Geneva, Switzerland, 2008

values below the noise level ($< 2\%$) of the diagnostic.

A continuous decrease in the electron density is observed in the core and edge line-integrated electron density signals even during the flat top of magnetic perturbation. A modest drop (a few per cent) in the total stored energy has been observed during the ELM control phase with the EFCCs. The electron density at the pedestal top decreases by $\sim 20\%$ due to so called density pump-out during the application of the $n = 1$ field, while the pedestal electron temperature increased what kept the pedestal pressure almost constant. However, the pedestal pressure gradient obtained from the derivative of the fitted curve shows that the maximum pressure gradient in the profile is decreased by $\sim 20\%$ during the application of the $n = 1$ field, and the edge pressure barrier is $\sim 20\%$ wider [18]. This is an effect mostly ascribable to the strong decrease in n_e pedestal height with an almost unvaried width. The power dependence of the mitigated ELM frequency has a same characteristic for type-I ELMs. However, the mitigated ELMs with $n = 1$ field have a higher frequency and are smaller in size. Reduction in ELM size with $n = 1$ field is inversely proportional to the increase in ELM frequency between the cases with $n = 1$ vs without $n = 1$ for all power levels.

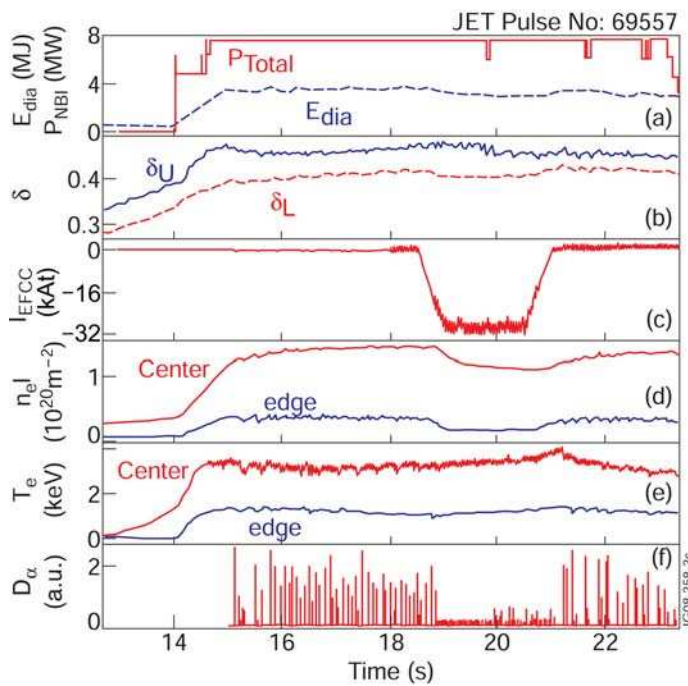


Figure 1 (a)-(f) Overview on a typical ELM control experiment in a high triangularity plasma. The traces are (a) the total input power, P_{tot} , and the total stored energy, E_{dia} , (b) upper and lower plasma triangularity, δ_U , δ_L , (c) I_{EFCC} , (d) the line-integrated electron densities n_eI , measured with an interferometer along two lines of sight, one close to the magnetic axis (upper trace) and the other near the pedestal top (lower trace) (the integration lengths of core and edge probing beams are ~ 3.2 m and ~ 1.5 m, respectively). The line lengths are reconstructed from a 2D EFIT equilibrium, (e) electron temperature in the core and near the pedestal top, (f) the D_α signal measured at the inner divertor.

The compensation of the density pump-out effect due to the application of the external $n = 1$ field has been demonstrated using gas puffing and pellet injection. The plasma density can be maintained during the flat top of I_{EFCC} by either of these two methods. An optimised gas fuelling rate to compensate the density pump-out effect without an additional drop in the plasma stored energy has been identified by means of gas fuelling up to a Greenwald fraction of 0.73 in low triangularity plasmas. Depending on the configuration of target plasmas the optimized gas fuelling rate can be different in value.

Differences in the particle flux, radiation, heat loads on outer divertor target between both methods for density pump-out compensation have been observed. In these experiments, the maximum deposited power per ELM reduced by about 35% with $n = 1$ field applied. When the density recovered by pellet injection, the maximum

deposited power per ELM reduced additionally while a weaker effect on the peak heat load in the same direction in the discharges with gas fuelling. During the inter-ELM phase, the average power deposited on targets reduces with pellet injection but increased with gas fuelling. The Average wetted area on target increased up to factor of 2 by both pellet injection and gas fuelling.

Recovery of the density and less effect on the total stored energy has been found with both those two methods in low density and low triangularity plasmas. However, compensation of density pump-out with pellet injection is faster than that with gas fuelling. Moreover, a less drop of electron temperature has been observed in the discharge with pellet injection when a density pump-out with $n = 1$ field is compensated as shown in figure 2.

Self-similar braking of plasma toroidal rotation, i.e. reduction of toroidal rotation in different radii by a same factor ($\Delta v_\phi/v_\phi = \text{constant}$), has been observed in the plasma core during application of EFCC fields in both, $n = 1$ and $n = 2$ configurations while a stronger braking appears at the plasma edge near the pedestal. There is a threshold value for the EFCC current which needs to be exceeded before the precursor frequency starts to decrease. The change of core plasma rotation does linearly depend on the amplitude of I_{EFCC} after the critical value (~ 12 kAt) has been exceeded. A similar magnitude of plasma braking has been observed with $n = 1$ and $n = 2$ fields when the same EFCC coil current was applied.

The torque profile of the perturbation field induced by the $n = 1$ EFCC current, T_{EFCC} , is determined by the momentum transport analysis using JETTO code. T_{EFCC} has a global profile and the maximum torque is at the plasma central region. The calculated NTV torque profile in the $1/\nu$ regime agrees with the profile of T_{EFCC} , although its absolute value is a factor of 2 larger. The NTV torque in the ν regime from the boundary layer contribution is comparable to the observed T_{EFCC} .

ELM control with a $n = 1$ field has been applied in low rotation plasmas with TF ripple

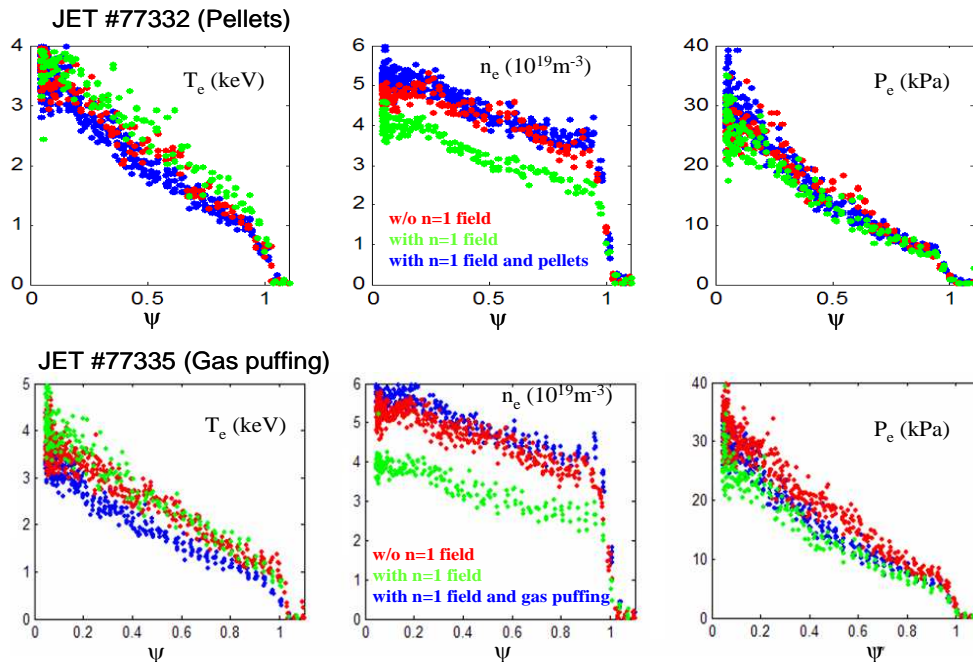


Figure 2 Radial profiles of electron temperature (left), density (middle) and pressure (right) measured in the phases without (red) and with (green) $n = 1$ field, and with additional fueling by pellet injection (Upper) and gas puffing (bottom).

up to 0.8%. The type-I H-mode target plasma ($I_p = 2.0$ MA; $B_t = 2.2$ T; $q_{95} = 3.6$) is maintained by NBI with $P_{\text{NBI}} = 10.8$ MW. The application of a $n = 1$ field with $I_{\text{EFCC}} = 32$ kAt leads to an increase of the ELM frequency in these plasmas with TF ripple. At large TF ripple of 0.5% and 0.8% the ELM character changes from type-I to compound ELMs because of less absorbed heating power with increasing fast ion losses. However, this compound ELMs became more regular small type-I ELM when a $n = 1$ field was applied.

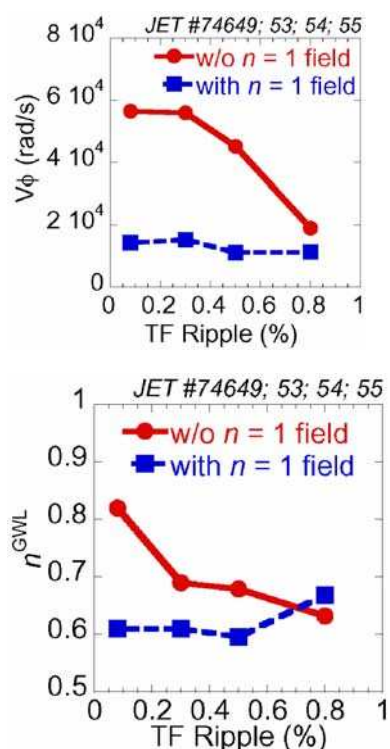


Figure 3 Plasma toroidal rotation at $R = 3.04$ m (left) and Greenwald fraction (right) as a function of TF ripple for the cases with and without $n = 1$ field.

Figure 3 (left) shows the plasma core toroidal rotation measured at $R = 3.04$ m by charge exchange spectrometry as a function of the TF ripple amplitude. With increasing ripple amplitude the plasma core rotation became smaller up to a factor of 3 when the TF ripple increased up to 0.8%. When a $n = 1$ field was applied, the plasma core rotation was reduced by a similar factor in plasmas with small ripple amplitude below 0.3%, while no additional change of plasma rotation was observed with a TF ripple amplitude above 0.8%. The plasma rotation braking with the $n = 1$ field does not depend on the TF ripple, and the plasma core rotation saturates. This result clearly shows the difference in plasma braking mechanism between TF ripple and a low n perturbation field. With application of the $n = 1$ field, the density drops by 20% in a plasma without additional TF ripple as shown in figure 3 (right). No additional density pump-out has been observed in plasmas with largest TF ripple of 0.8%. Both, TF ripple and low n perturbation fields, cause density pump-out, however, the experimental result suggests a different mechanism of both cases. This result also demonstrate the final saturation value due to the density pump-out effect of the low- n field does not depend on the density of the target plasma, which is not understood yet based on the existing theory.

Summary Recently, ELM control experiments have been performed on JET aiming at understanding the plasma response on the magnetic perturbation. Firstly, compensation of the density pump-out effect of perturbation field has been achieved by means of gas fuelling up to a Greenwald fraction of 0.73 in low triangularity plasmas, and by pellets fuelling. Secondly, ELM control has been also carried out in slower rotating plasmas with toroidal field (TF) ripple. A clear difference in the effects on the plasma rotation and density pump-out between TF ripple and EFCC was observed.

Acknowledgement This work, supported by the European Communities under the contract of Association between EURATOM and Belgian State, was carried out within the framework of the European Fusion development Agreement. The views and opinions expressed herein do not necessarily reflect those of the European Commission.